Journal of Bioresources and Bioproducts 9 (2024) 43–57

Contents lists available at ScienceDirect

Journal of Bioresources and Bioproducts

journal homepage: https://www.keaipublishing.com/en/journals/journal-of-bioresources-and-bioproducts/

Research Article

The *Pichia pastoris* enzyme production platform: From combinatorial library screening to bench-top fermentation on residual cyanobacterial biomass

Korbinian Sinzinger[a,1], Ulrike Obst[a,1], Samed Güner[a], Manuel Döring[a], Magdalena Haslbeck[a], Doris Schieder[a,*], Volker Sieber[a,b,c,d]

[a] *Chair of Chemistry of Biogenic Resources, Campus Straubing for Biotechnology and Sustainability, Technical University of Munich, Straubing 94315, Germany*
[b] *Catalysis Research Center, Technical University of Munich, Garching 85748, Germany*
[c] *SynBiofoundry@TUM, Technical University of Munich, Straubing 94315, Germany*
[d] *School of Chemistry and Molecular Biosciences, The University of Queensland, St. Lucia 4072, Australia*

ARTICLE INFO

Keywords:
Protein secretion
Phytase
Cyanobacterial biomass
Fed-batch fermentation
Pichia pastoris

ABSTRACT

The demand for industrial enzymes is continually rising, fueled by the growing need to shift towards more sustainable industrial processes. However, making efficient enzyme production strains and identifying optimal enzyme expression conditions remains a challenge. Moreover, the production of the enzymes themselves comes with unavoidable impacts, e.g., the need to utilize secondary feedstocks. Here, we take a more holistic view of bioprocess development and report an integrative approach that allows us to rapidly identify improved enzyme expression and secretion conditions and make use of cyanobacterial waste biomass as feed for supporting *Pichia pastoris* fermentation. We demonstrate these capabilities by producing a phytase secreted by *P. pastoris* that is grown on cyanobacterium hydrolysate and buffered glycerol-complex (BMGY) medium, with genetic expression conditions identified by high-throughput screening of a randomized secretion library. When our best-performing strain is grown in a fed-batch fermentation on BMGY, we reach over 7 000 U/mL in three days.

1. Introduction

The transition to a sustainable global society requires greener industrial production processes, including the biochemical valorization of biomass as renewable feedstock. Integrated multi-product biorefinery concepts are needed to overcome the hurdles for profitable commercialization. In a biorefinery concept, biomass is converted efficiently into multiple marketable products, such as fuels, chemicals or enzymes. Among others, this requires a multi-field research approach to handle the complex interplay of developing microbial hosts that can convert residual biomass to valuable products, upcycling a feed to make it accessible for the hosts and engineering the hosts to produce valuable products.

Microalgae and cyanobacteria are a promising renewable feedstock for fermentation processes that deliver high-value compounds (Chandra et al., 2019; Mitra and Mishra, 2019; de Farias Silva et al., 2019). These photosynthetic microorganisms can grow and multiply using light as energy and CO_2 as a carbon source (Chandra et al., 2019). They are characterized by their more rapid growth compared to terrestrial plants and do not require arable land or freshwater; hence don't compete with plant-based food or feed

* Corresponding author.
E-mail address: doris.schieder@tum.de (D. Schieder).
[1] Korbinian Sinzinger and Ulrike Obst contributed equally to this work and should be considered co-first authors.

https://doi.org/10.1016/j.jobab.2023.12.005

Available online 26 December 2023

(de Farias Silva et al., 2019). Cyanobacteria are Gram-negative prokaryotes with a structured cell envelope, but their cell wall contains a peptidoglycan layer, which more closely resembles that of Gram-positive bacteria. Hence, carbohydrates entrapped within the cell wall or stored intracellularly in the form of starch/glycogen are easily degraded by enzymatic hydrolysis and accessible as fermentation substrates (Choi et al., 2010; Möllers et al., 2014). Here, we use the previously investigated biomass of the cyanobacterium species *Nostoc* sp. De1 to produce an enzymatic hydrolysate suitable for fermentation (Sinzinger et al., 2022). However, challenges exist due to the filamentous growth and the presence of bioactive components in *Nostoc* colonies, necessitating the selection of a robust organism for fermentation (Briones-Nagata et al., 2007).

The *Pichia pastoris* (*Komagataella phaffii*) is a methylotrophic yeast known for its robustness and widespread use in protein production processes for various applications. Its advantages include microbial safety, rapid growth to high-cell densities, and ease of genetic manipulation. The *P. pastoris* supports efficient protein secretion, allowing for complex folding processes and facilitating downstream purification (Delic et al., 2013; Zang et al., 2021). Despite extensive engineering efforts of the yeast secretion system, process development remains challenging due to many cross-reacting factors. We focused on the expression and secretion of phytases, crucial enzyme additives in animal feed, which hydrolyze phytate ester bonds, improving phosphate and mineral uptake and reducing environmental pollution (Chen et al., 2015). The phytase market has exceeded 300 million US dollar and continues to grow about 10 % per year with an ongoing interest in enhancing the substrate specificity, catalytic efficiency, and thermostability to improve the pH profile and reduce production costs (Chen et al., 2015; Herrmann et al., 2019). Phytases aimed for the feed and food industry are sold from 1 to 5 US dollar per kg (David, 2018).

Variant libraries using differing genetic designs are usually screened to identify suitable protein expression and secretion conditions. To assist in the design of *P. pastoris* secretion libraries, we previously developed a toolkit of regulatory elements (PTK), which included promoters, secretion signal peptides, and a terminator (Obst et al., 2017). Standardization was key to ensuring parts were interchangeable for creating randomized libraries and multi-component systems (Canton et al., 2008). The PTK follows the widely used Modular Cloning (MoClo) design rules of the *Saccharomyces cerevisiae* Yeast toolkit (YTP) (Lee et al., 2015). Rajkumar et al. (2019) further expanded the number of interchangeable parts available with their toolkit specific for *Kluyveromyces marxianus*, enabling 552 options for a gene to be expressed intracellularly and over 55 000 possibilities if secreted (when these three matching toolkits are combined). Additional expression options arise when parts from other toolkits with different designs are considered, e.g., the promoter toolbox from Vogl et al. (2016), the GoldenPiCS toolkit from Prielhofer et al. (2017), or the secretion toolkits for other methylotrophic yeast from Celińska et al. (2018) for *Yarrowia lipolytica* and from Yarimizu et al. (2015) for *K. marxianus*. The challenge that arises from using these libraries is the lack of methods to screen the resultant designs efficiently for *P. pastoris* because the construction and evaluation of each design individually would be too slow and costly to perform.

Here, we studied four different phytases that previously were successfully expressed in *P. pastoris*: three fungal phytases (PhyA) from *Aspergillus niger* (Han and Lei, 1999), *Thielavia heterothallica* (Ranjan and Satyanarayana, 2016), *Peniophora lycii* (Xiong et al., 2005) and a bacterial phytase (periplasmic phosphoanhydride phosphatase, AppA) from *Escherichia coli* (Akbarzadeh et al., 2015). We took a comprehensive approach, considering all major factors for enzyme production by *P. pastoris* in buffered glycerol-complex (BMGY) medium and showing a proof of principle process that uses cyanobacterial biomass as feedstock. An overview of the study is given in Fig. 1, outlining the process from library design and screening to fed-batch fermentation. We tackled the bottleneck of screening by developing a combinatorial library to facilitate easy *P. pastoris* engineering. The workflow comprised three main steps: plasmid library assembly from toolkit plasmids using Golden Gate shuffling (Engler et al., 2009), yeast transformation and colony isolation, and library screening for identifying best performs. In addition, we demonstrated the successful fermentation of *P. pastoris* in *Nostoc* sp. De1 hydrolysate for AppA *E. coli* phytase expression in flasks and 1 L bench top scales. In the 1 L reactor system, we determine the strain-specific growth kinetics in batch and pulsed batch fermentation in BMGY medium and finally develop a fed-batch fermentation strategy in BMGY medium concluded by a process evaluation.

This is the first time the PTK has been used to generate a diverse library of expression constructs to optimize a broader bioprocess that is able to utilize a sustainable feedstock. It also demonstrates the ability for *P. pastoris*, an industrial workhorse, to productively grow on cyanobacterium hydrolysate, enabling a new source for sustainable bioproduction. More broadly, this work highlights the innovation that is possible when combining technologies from synthetic biology, microbiology, and bioprocess development to create end-to-end solutions for challenging problems.

2. Material and methods

2.1. *Chemicals,* Nostoc *biomass and enzymes*

All chemicals were, unless otherwise stated, purchased in analytical grade from Sigma Aldrich (Germany), Merck KGaA (Germany) and Carl Roth GmbH (Germany). Freeze dried whole cells from *Nostoc* sp. De1 was kindly provided by Centre Algatech, Institute o f Microbiology, The Czech Academy of Sciences (Třeboň). The following enzyme mixtures were used: DISTILLASE® CS (amyloglucosidase & α-amylase) and FERMGEN^{TM} (protease) from Genencore, and Viscozyme® L (cellolytic) purchased from Sigma Aldrich.

2.2. *The DNA plasmids and molecular cloning*

Part plasmids used in this study originated from either the Yeast Toolkit (YTK, Addgene Kit: 1000000061, Cambridge, MA, USA) (Lee et al., 2015), the PTK (Addgene Kit: 1000000108) (Obst et al., 2017), were ordered from Twist Bioscience (Santa Clara, CA, USA)

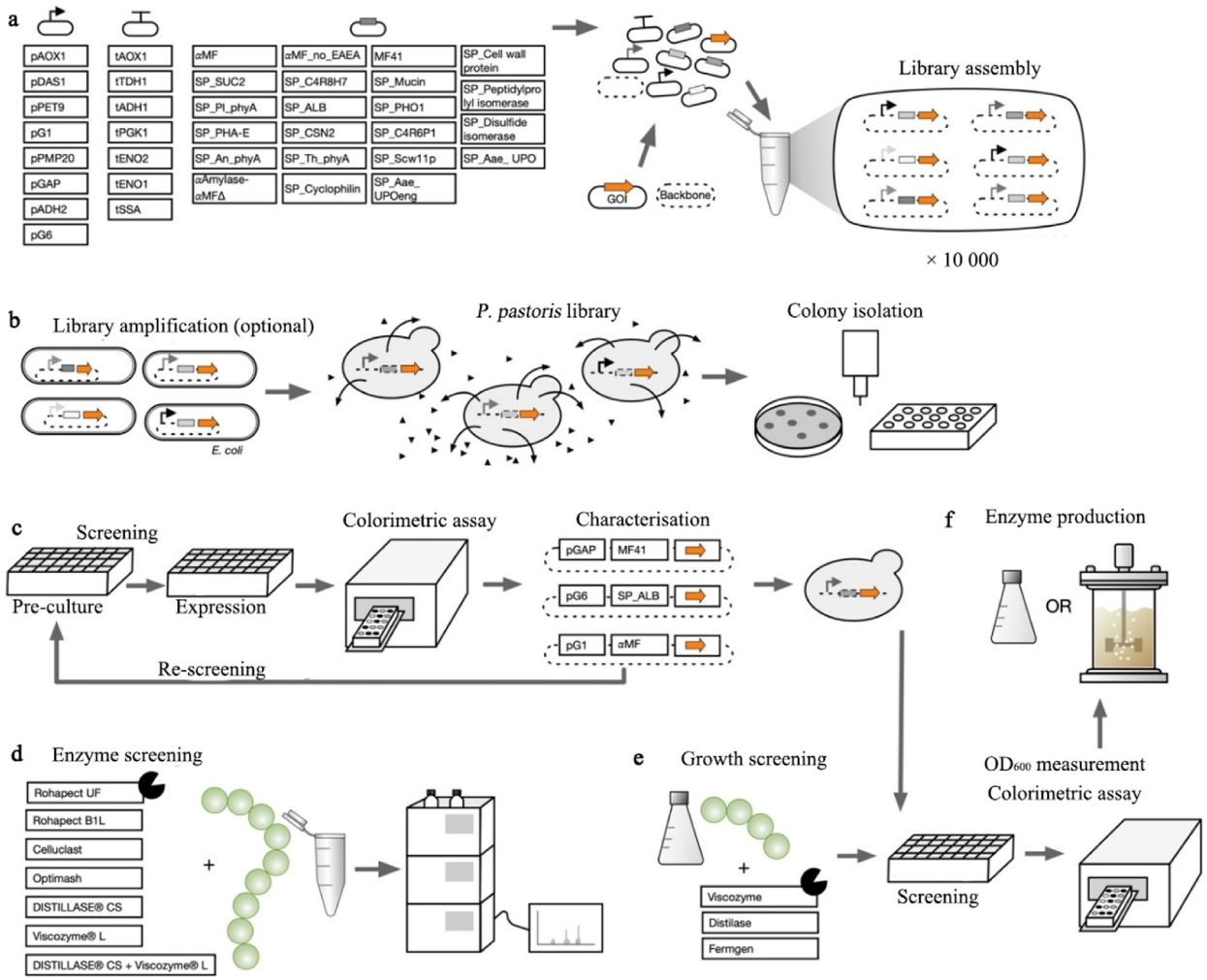

Fig. 1. Overview of work conducted in this study. (a) development of a combinatorial library to facilitate easy *Pichia pastoris* engineering; (b) characterization of the library components. (c) library screenings for industrially relevant phytase enzyme production; (d) investigate preparation of enzymatic hydrolysate from *Nostoc* sp. De1 biomass; (e) demonstration of successful fermentation of *P. pastoris* in this hydrolysate for periplasmic phosphoanhydride phosphatase (AppA) *Escherichia coli* phytase expression; (f) development of a fed-batch fermentation strategy in a 1 L format.

or were constructed by standard molecular cloning techniques. Constructed part plasmids were made with gene fragments (Twist Bioscience) or polymerase chain reaction (PCR) fragments integrated into the pYTP001 backbone vector using Golden Gate assembly with enzymes from New England BioLabs (Beverly, Massachusetts, USA).

Expression libraries were built from part plasmids encoding each functional element and inserted into the backbone vector pPTK051 (made in this study, 4 327 bp in size). Assembly was performed using a Golden Gate reaction (37 ˚C, 10 min; 50 × (37 ˚C, 5 min; 16 ˚C, 5 min); 37 ˚C, 10 min; 65 ˚C, 10 min) with T4 ligase and BsaI (Engler et al., 2009). The total concentration of each insert was twice that of the backbone vector pPTK051. For the generation of randomized libraries via shuffling, the DNA concentration of each insert was the total amount of insert divided by the number of plasmids used in the assembly. For example, when using 300 fmol of insert and three different plasmids for shuffling, 100 fmol of each plasmid was used in the assembly.

For the phytase shuffling, an assembly reaction was assembled containing: 20 secretion signals, a terminator part and a linearized backbone from the PTK. This was split into two equally sized reactions to which the respective promoter parts for induced (pAOX1, pDAS1, pPMP20) and constitutive (pGAP, pPET9, pG1, pG6, pADH2) expression were added. These reaction mixes were then each split again into 4 reactions to which the phytases were added. The final reaction mixtures contained: 50 fmol backbone, 100 fmol for each functional part, restriction enzyme, and T4 ligase. Following the Golden Gate reaction, *E. coli* DH5*α* (Thermo Fisher Scientific, Waltham, MA, USA) or NEB Turbo (New England Biolabs, Ipswich, MA, USA) cells were chemically transformed and grown in lysogeny broth (LB) with relevant antibiotics (25 mg/mL chloramphenicol, 30 mg/mL kanamycin sulfate).

2.3. *The* P. pastoris *strain and transformation*

For *P. pastoris attP* (NRRL Y-11430 + *attP* recombinase target site) transformation, competent cells were prepared as described by Madden et al. (2015) and stored at –80 ˚C until use. Competent cells were combined with 200–500 ng of the BxbI plasmid (Perez-Pinera et al., 2016) and 200–500 ng of the circular expression vector in a 1 mm electroporation cuvette. The reaction mixture was then pulsed at 1 800 V, 25 μF, 200 Ohm (Micro Pulser Electroporator, Bio-Rad Laboratories GmbH, München, Germany) and 1 mL *Pichia* electroporation recovery solution (PERS, 50 % (*V/V*) yeast extract peptone dextrose (YPD), 50 % (*V/V*) 1 mol/L sorbitol) was added. Everything was then transferred into a 2 mL cup for recovery through growth at 30 ˚C, 100 r/min for 3.5 h. Following this, 100 μL of the cell solution and the cell pellet (8 000 r/min, 30 s; Heraeus Fresco 21 Centrifuge, Thermo Fisher Scientific, Waltham, MA, USA) were plated on YPD media (2 % peptone, 2 % glucose and 1 % yeast extract) containing 75 μg/mL zeocin. The Golden Gate reaction was used directly for *P. pastoris* transformation for strains pUO_pL730–pUO_pL771. Red fluorescent protein (RFP) and yeast-enhanced green fluorescent protein (yEGFP) expression strains previously prepared were used for Reference Obst et al. (2017).

2.4. *The* P. pastoris *cultivation condition*

General *P. pastoris* growth was carried out using YPD media. For protein expression, cells were grown in either buffered glycerol/methanol-complex (BMGY/BMMY) or buffered minimal dextrose/methanol (BMD/BMM) media with modifications. Zeocin was added (75 μg/mL final concentration) to the media except when assessing the growth of the wild-type strain.

2.4.1. *Strain characterizations and screening*

The screening was performed in 96-well deep-well plates with incubation at 30 ˚C and 900 r/min (Weis et al., 2004). Pre-cultures were inoculated using an automated colony picker (Norgren Systems, Fairlea, WV, USA) from glycerol stocks and grown for 48 h. Constitutive or induced expression cultures were inoculated from this pre-culture using an automated liquid handling platform (Tecan Group Ltd., Männedorf, Switzerland; MCA96 multi-channel arm). While the expression plates were incubated, methanol was added to induce expression in the cultures every 24 h to ensure 1 % (*V/V*) methanol was maintained throughout.

The RFP and yEGFP expression was monitored as described in Qin et al. (2011). Specifically, 900 μL of 0.2 % BMD glucose pre-culture consisting of 100 mmol/L potassium phosphate, 1.34 % (*w/V*) yeast nitrogen base, 0.000 04 % (*w/V*) biotin, 0.2 % (*w/V*) glucose was inoculated manually from a glycerol stock. The expression culture in 1 % BMD glucose (100 mmol/L potassium phosphate, 1.34 % (*w/V*) yeast nitrogen base, 0.000 04 % (*w/V*) biotin, 1 % (*w/V*) glucose) or 1 % BMM methanol (100 mmol/L potassium phosphate, 1.34 % (*w/V*) yeast nitrogen base, 0.000 04 % (*w/V*) biotin, 1 % (*w/V*) methanol] was inoculated with 30 μL of the pre-culture and incubated for 48 h before measurements were taken.

The phytase screening was performed as in Hesampour et al. (2015). Specifically, a 96-well agar plate was used to inoculate 1.2 mL pre-culture, of which 100 μL was used as inoculant for 900 μL of the expression-culture. This was then incubated for 48 h. For inducible expression, the pre-culture was 2 % BMGY-PP (BMGY-phosphate buffer, 1 % (*w/V*) yeast extract, 2 % (*w/V*) peptone, 1.34 % (*w/V*) yeast nitrogen base, 0.000 04 % (*w/V*) biotin, 2 % (*V/V*) glycerol), the expression-culture 1 % BMMY-PP [1 % (*w/V*) yeast extract, 2 % (*w/V*) peptone, 1.34 % (*w/V*) yeast nitrogen base, 0.000 04 % (*w/V*) biotin, 1 % (*V/V*) methanol]. For methanol induction, 10 % BMMY-PP (1 % (*w/V*) yeast extract, 2 % (*w/V*) peptone, 1.34 % (*w/V*) yeast nitrogen base, 0.000 04 % (*w/V*) biotin, 10 % (*V/V*) methanol] was added after 24 h of expression to maintain 1 % (*V/V*) methanol throughout the experiment. For constitutive expression, the pre-culture was 0.4 % BMGY-PP (1 % (*w/V*) yeast extract, 2 % (*w/V*) peptone, 1.34 % (*w/V*) yeast nitrogen base, 0.000 04 % (*w/V*) biotin, 0.4 % (*V/V*) glycerol) and the expression-culture 2 % BMGY-PP. To determine OD_{600} and create cryo-cultures, 180 μL 16.66 % (*V/V*) glycerol was mixed with 20 μL sample in flat bottom assay plates, OD_{600} was measured (Infinite 200 pro microplate reader, Tecan Group Ltd., Männedorf, Switzerland), and plates were stored at –80 ˚C.

2.4.2. *Shake flask experiments*

The *P. pastoris* cultivation was done in 50 mL shake flasks, starting with 10 mL pre-culture of 0.4 % BMGY (from here on forth -PP) for 48 h at 30 ˚C and 150 r/min inoculated from an agar plate. The 10 mL expression cultures in BMGY/BMD or pure hydrolysate with 2 % (*w/V*) glycerol or glucose were inoculated with 1 mL of pre-culture and again incubated for 48 h at 30 ˚C and 150 r/min. The OD_{600} was measured using an Ultraspec 10 spectrophotometer (Amersham Bioscience, UK). The cultures were transferred to 15 mL Falcon® tubes and subsequently the samples were centrifuged at 500 × g for 10 min. The supernatants were then analyzed with the Bradford assay using bovine serum albumin (BSA) as standard for protein content and the phytase activity was determined as described below.

2.4.3. *Batch and fed-batch fermentation*

All fermentations were conducted in 1 L DASGIP® bioreactors (Eppendorf, Germany) with an initial volume of 500 mL 4 % BMGY and at 30 ˚C. For the pulsed batch, 25 mL of 50 % (*w/V*) glycerol was injected once after 12 h with a syringe into the sample port and flushed once with sterile air. Fed-batch fermentations were continuously fed with a total amount of 200 g of 50 % (*w/V*) glycerol depending on the strategy. The stirrer was equipped with a 6-plate-rushton impeller placed 2.5 cm from the bottom of the shaft stirring with an initial rate of 400 r/min. Maximum stirring rate was initially 1 200 r/min, which was reduced to 900 r/min for optimized fermentations. Batch and pulsed batch fermentations were performed with an aeration of 0.2–0.5 ($m^3/(m^3 \cdot min)$). Fed-batch fermentations were performed additionally with 0.5–1.2 ($m^3/(m^3 \cdot min)$). Agitation and aeration were automatically adjusted to maintain the level of dissolved oxygen over 30 %. The pH was maintained at 5.0 and automatically adjusted with 20 % NH_4OH

(directly into the broth) or with 7 % H_2SO_4 as required. Foam control was done using 1 % antifoam B (Merk, Germany). For monitoring process parameters, the reactors were equipped with probes for pH and dissolved oxygen. The 3 mL samples were taken every 3–5 h. Cell growth was determined as above; cell dry weight was determined by centrifuging 1 mL cell culture broth at 500 × g for 10 min and drying the cell pellet overnight at 105 °C. The supernatant was analyzed for glycerol after 1:10 dilution in 2.5 mmol/L H_2SO_4 and filtration (0.2 μm, PVDF) by high-performance liquid chromatography-RID (Dionex Corp., USA, RI 101, Shodex, Tokyo, Japan) equipped with an Rezex ion exclusion column (Rezex ROA-Organic Acid H+ (8 %); 300 mm × 7.8 mm; Phenomenex Deutschland Ltd.). The column oven temperature was set to 70 °C, and 2.5 mmol/L sulfuric acid was used for isocratic elution at a flow rate of 0.5 mL/min. Later the phytase activity was determined as described in Section 2.6. The OD_{600}, DCW, and phytase activity values in the fed batch fermentations were normalized to the starting volumes.

2.5. Fluorescence assay for RFP and yEGFP determination

To measure fluorescence, 100 μL culture or supernatant after centrifugation at 4 °C and 500 × g for 10 min were used, and intensity was normalized to OD_{600}, if not otherwise stated. To determine OD_{600}, samples were diluted in phosphate-buffered saline (PBS) buffer, pH 7.4. The parental *P. pastoris* strain not expressing the fluorescent protein was assayed in parallel and used to determine background fluorescence, which was averaged over all parent strains and removed from the fluorescence of the expression strains.

2.6. Colorimetric assay determining phytase activity

Phytase activity was measured using a colorimetric assay by monitoring the free phosphate released from phytate with ammonium molybdate. First, the culture was centrifuged (4 °C, 500 × g, 10 min) and the secreted protein in the supernatant was purified via gel-filtration using 96-Well SpinColumns (25–100 μL) (Harvard Apparatus, Holliston, MA, USA). Columns were centrifuged at room temperature at 2 000 × g for 2 min, before being hydrated with 200 μL water per well for 20 min and subsequently centrifuged as before. Each of these columns was then washed three times with 150 μL water. During this step, the first two centrifugations were at 2 000 × g and the final one at 1 000 × g (room temperature (RT), for 2 min). To purify the secreted proteins, 35 μL of the supernatant was loaded into wells and the plate was centrifuged (RT, 1 000 × g, 2 min) to collect the filtrate.

Finally, phytase activity was quantified using the method of Bae et al. (1999), but adapted to higher-throughput (i.e., 96-well-plates). Specifically, 13.5 μL gel filtrate, or water dilutions thereof, were combined with 53.5 μL of phytate substrate solution (1.5 mmol/L sodium phytate in 0.1 mol/L sodium acetate buffer, pH 5.0 using acetic acid) in a 96-well plate and incubated at 37 °C for 30 min. The 66.6 μL of a stop solution (5 % (*w/V*) trichloroacetic acid (TCA)) was added to terminate the reaction, followed by 66.6 μL of coloring solution (4 volumes reagent A (1.5 % (w/v) ammonium molybdate, 5.5 % (v/v) sulfuric acid solution) and 1 volume of reagent B (2.7 % (*w/V*) ferrous sulfate)). To calculate phytase units (U), potassium phosphate from 0.8 to 20 mmol/L was measured alongside each plate for the screening and up to 5 mmol/L for all other experiments. Absorbance at 700 nm was then measured.

2.7. Hydrolysate production

The *Nostoc* sp. De1 hydrolysate production was done in a 500 mL shaking flask. 5 % (*w/V*) of *Nostoc* sp. De1 biomass was suspended in 100 mL of 50 mmol/L citrate buffer pH 4.5. The biomass was pre-treated at 80°C for one hour. After cooling down, 0.05 % (v/v) DISTILLASE® CS and Viscozyme® L were added for saccharification for 24 h at 50 °C, while shaking at 150 r/min. After allowing it to cool again, 0.05 % (*V/V*) FERMGEN™ was added for solubilization over another 36 h at 30 °C and shaking at 150 r/min. Subsequently, the treatment ended by a heating step: 90 °C for 30 min in a preheated oven. The biomass slurry was then transferred into 500 mL centrifugation buckets and spun with 8 000 × g for 30 min at RT. The supernatant was sterile filtered (0.2 μm) into a sterile flask and kept at 4 °C until further use.

3. Results and discussion

3.1. Characterization of extended PTK

To develop an optimal phytase production host, we first extended our previous PTK (Obst et al., 2017) with 25 additional regulatory elements from *P. pastoris* (6 promoters, 19 secretion tags) and tested another 13 parts from the YTK (Lee et al., 2015) (7 promoters, 6 terminators). For characterization, we used a red fluorescent protein (RFP) and a yeast-enhanced green fluorescent protein (yEGFP) as reporters, which allowed for the simple measurement of bulk fluorescence (Fig. 2).

For higher product yields and precise tuning of gene expression, we tested the promoters for intracellular expression levels of RFP and yEGFP. We studied two strong methanol inducible promoters (pDAS1 (Vogl et al., 2016), pPMP20 (Vogl et al., 2016)), four constitutive promoters (pPET9 (Stadlmayr et al., 2010), pG1 (Prielhofer et al., 2013), pG6 (Prielhofer et al., 2013), pADH2 (Vogl et al., 2016)) and seven *S. cerevisiae* YTK promoters for their applicability in *P. pastoris* (pTDH3, pCCW12, pHHF2, pTEF2, pHHF1, pHTB2, pRPL18B) (Lee et al., 2015). We compared the intracellular expression levels of RFP and yEGFP from genomically integrated expression constructs (Fig. 2a). The newly added *P. pastoris* promoters resulted in high expression levels, both for GFP and RFP. The newly tested *S. cerevisiae* promoters, except for pTDH3 all promoted protein expression in *P. pastoris*. However, we did see better expression for RFP over yEGFP. Therefore, we selected the endogenous promoters for screening phytase production strains as they result in stronger expression levels and cover the desired spectrum of expression strengths.

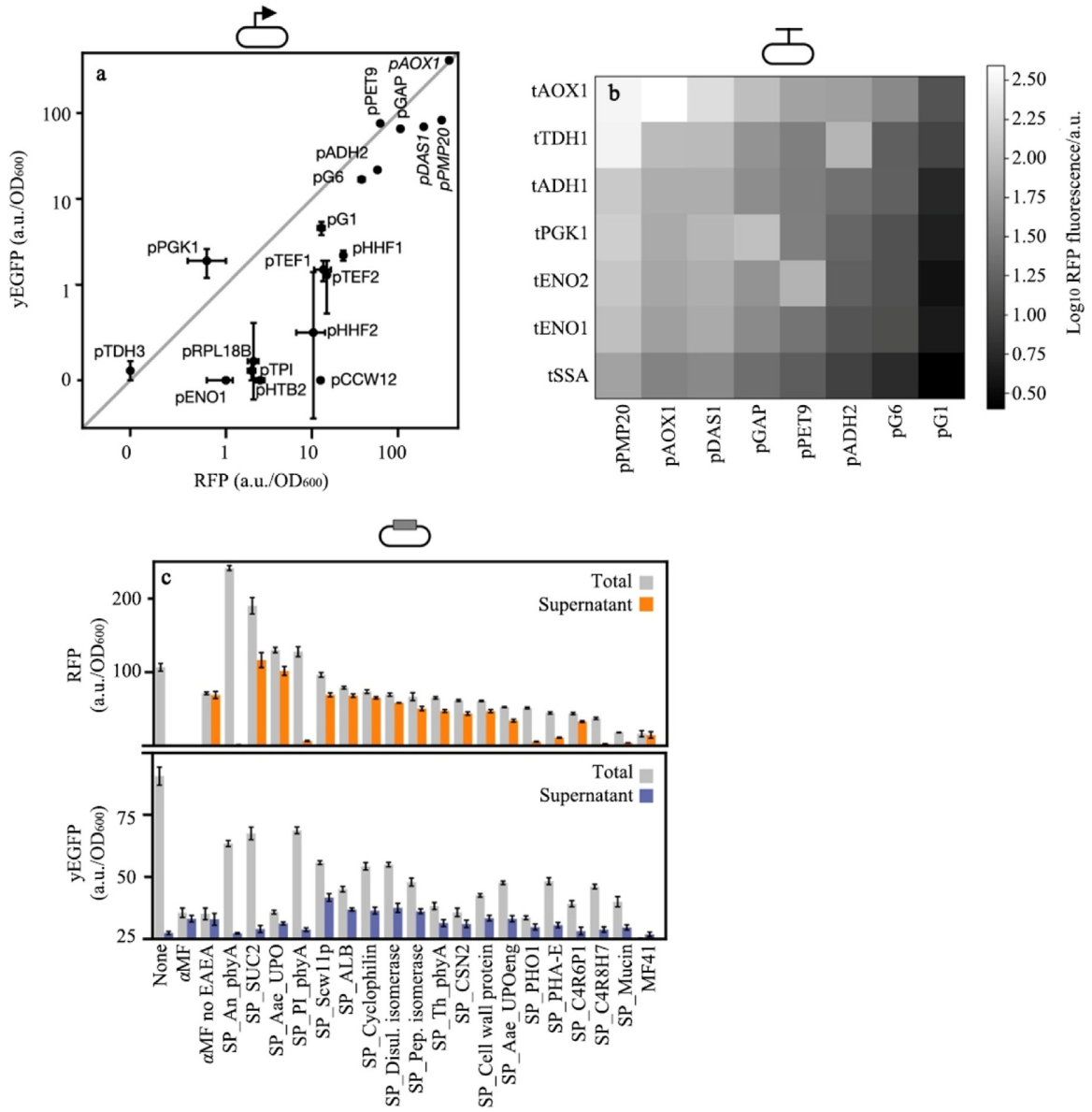

Fig. 2. Characterization of extended *Pichia* Toolkit (PTK) and additional Yeast Toolkit (YTP) regulatory elements. (a) relative promoter strength was evaluated for intracellular red fluorescent protein (RFP) and yeast-enhanced green fluorescent protein (yEGFP) expression. (b) characterization of promoter-terminator combinations. Heat map of RFP fluorescence values given in a.u. (fluorescence normalized to OD_{600}) in a logarithmic scale. (c) for secretion analysis, tags under the control of the constitutive promoter pGAP were analysed for RFP and yEGFP expression and secretion. For all samples, the total fluorescence, as well as the fluorescence of the supernatant after centrifugation, was determined. Three biological replicates were analysed, and the mean fluorescence normalized to the OD_{600} (a.u./OD_{600}) is presented with error bars that denote ± 1 standard deviation. Characterization was performed in 1 % buffered Minimal Methanol (BMM) for the inducible promoter pAOX1 and 1 % buffered minimal dextrose (BMD) for all other constitutive promoters. (For interpretation of the references to color in this figure, the reader is referred to the web version of this article).

In *S. cerevisiae* the terminator is important in tuning protein expression by up to 35-fold through impacts on mRNA stability (Curran et al., 2013; Morse et al., 2017). In *P. pastoris* terminators studied by Vogl et al. (2016) showed only minor differences in expression levels when different terminators were used. Here, eight *P. pastoris* promoters were coupled to six different YTK terminators (tTDH1, tADH1, tPGK1, tENO2, tENO1, tSSA1) or the *P. pastoris* terminator tAOX1 (Fig. 2b) to drive intracellular expression of RFP and test this idea further. We found that terminator choice significantly impacted expression levels by up to 5-fold across the promoter-terminator combinations, except for when the pAOX1 promoter was used where differences up to 10-fold were observed. Terminators were sorted according to their ability to tune expression for each promoter with tAOX1 typically causing higher expression levels,

and tSSA1 negatively impacting expression strength. This ranking was found to be similar for almost all promoters (other than the combinations: pGAP-tPGK1, pPET9-tENO2, pADH2-tTDH1), suggesting a systematic effect underlies the changes.

In eukaryotes, protein secretion primarily occurs via the endoplasmic reticulum (ER)—Golgi pathway, requiring a signal peptide on the N-terminal of the nascent polypeptide for translocation through the ER membrane (Delic et al., 2013; Liang et al., 2013). To fine-tune secretion, we included an additional 9 endogenous *P. pastoris*, 8 exogenous and 2 synthetic signal peptides to our toolkit. We selected tags based on previous knowledge regarding signal peptides and their prediction and initial signal peptide characterization was performed using RFP and yEGFP controlled by the strong constitutive promoter pGAP. Fluorescence of the total culture and supernatant were measured and OD_{600} was normalized (Fig. 2c). The secretion efficiency of the signal sequences varied for the reporter proteins RFP and yEGFP, as previously seen for synthetic tags (Obst et al., 2017), highlighting the importance of the signal peptide and gene of interest (GOI) combination when designing a secretion system. Here, we found that more RFP is expressed for the signal peptides SP_An_phyA, SP_SUC2, SP_Aae_UPO, or SP_Pl_phyA., while only SP_SUC2 and SP_Aae_UPO enabled higher secretion efficiencies than the commonly used mating factor α αMF_no_EAEA signal peptide. For yEGFP, the highest expression is seen for the intracellular expression construct without a tag. In comparison to the widely used αMF_no_EAEA or αMF signal peptides, higher secretion levels are achieved when using SP_Scw11p, SP_ALB, SP_Cyclophilin, SP_Disulfideierase, SP_Cell wall protein, SP_Peptidylprolyl isomerase and SP_Aae_UPOeng. Comparing endogenous *P. pastoris* or exogenous signal peptides, there is no noticeable difference. The analysis of the six newly characterized signal peptides shows two (SP_Cyclophilin and SP_Th_phyA) induce efficient secretion, two (SP_An_phyA, SP_Pl_phyA) lead to overall very high protein ex but no secretion, and two (SP_C4R8H7, SP_Mucin) result in only low amounts of secreted RFP and yEGFP. These results demonstrate the functionality of the newly designed regulatory elements and provided insight for part choice during the phytase screening.

3.2. Application of extended PTK on phytase expression

A selection of the extended PTK was used to generate randomized libraries to screen for beneficial combinations of regulatory elements for the phytase genes to achieve high levels of secreted phytases. All sequences were codon optimized for *P. pastoris* and designed to be compatible with the PTK. Secretion libraries with 20 secretion tags for induced and constitutive expression (3 and 5 different promoters, respectively) were made for each phytase. To cover the 60 or 100 possible combinations for the induced and constitutive library, respectively, 182 and 364 *P. pastoris* strains were screened to achieve an expected coverage of at least 95 %. Suitable screening conditions were established and validated (Fig. 1), to differentiate positive hits (active enzyme expression) from negative variants (no expression or inactivity of the enzyme). Expression supernatant after centrifugation was purified to remove small molecules via gel-filtration chromatography and a colorimetric assay was used to determine phytase activity using absorption measurements at 700 nm.

For all phytase screenings, strains producing active enzymes were identified, but the activity level and amount of secreted protein varied significantly. For each phytase, the activity landscape showed similarities between constitutive and induced screening. The decreasing activity for the *A. niger* and *P. lycii* phytases indicates a clear preference for specific promoter and secretion tag combinations. The smaller decrease (with many strains showing high activity) for the *E. coli* phytase suggests that this protein has less of an effect on the performance of the promoter and tag choice. A selection of strains for each library was re-screened, to confirm the initial results. The best performing from the induced and constitutive screening (10 and 22 colonies, respectively) and colonies that were found to not express any phytase (3 and 5 colonies, respectively), and were plated onto fresh agar media. Biological triplicates were screened and for a selection of strains, the genotype of the expression construct was found using sequencing (Fig. 3).

For each phytase, specific tags were found to support secretion better than others, while some were non-functional for all of the phytases tested. To assess this in more detail, 60 of the strains were sequenced. Of these, only six of the tags were not seen in any strain (three phytase signal peptides SP_Pl_phyA, SP_An_phyA, SP_Th_phyA; and signal peptides αAmylase–αMFΔ, SP_SUC2 and SP_PHA-E). For secretion of both fluorescent proteins, we found that both SP_An_phyA and SP_Pl_phyA were also non-functional. This suggests that *P. pastoris* may not be able to recognize these heterologous tags for secretion. The other four tags were shown to enable secretion of the fluorescent proteins previously (Fig. 2c), however, their function could be impacted by the phytase. The tag SP_PHO1 stood out, for its efficient secretion for all constitutive phytase expression strains. In addition, specific secretion tag-phytase combinations seemed to be beneficial. For example, SP_C4R8H7 for *A. niger* and *T. heterothallica*, SP_Mucin for *P. lycii*, and MF41 or the related αMF and αMF_no_EAEA tags for *E. coli*. When the gene was constitutively expressed, we found that the pGAP promoter gave the strongest expression, except for when the *P. lycii* phytase was used, where pG6 and pAHD2 resulted in the highest expression. For these constitutively expressed variants, only the pPET9 promoter did not appear in the sequencing data. For the designs using an inducible promoter, all three were found to lead to strong phytase expression, with pAOX1 and pPMP20 often outperforming pDAS1 as also seen for fluorescent proteins (Fig. 2a).

In summary, our screening identified functional promoter and tag combinations for each phytase. However, the number of suitable combinations varied significantly for each phytase and the secretion efficiency was heavily influenced by the combination of promoter, tag, and gene of interest. This illustrates the need for effective screening tools (Prielhofer et al., 2017). The novel tags SP_C4R8H7 and SP Cyclophillin, or the less commonly used tags SP_CSN2 and SP_PHO1 performed well in many contexts and could provide a suitable alternative to the most widely used tag αMF (Massahi and Çalık, 2015). For example, the application of SP_CSN2 instead of αMF increased the amount of secreted *A. niger* phytase by 20 % providing a simple to apply means for strain improvement.

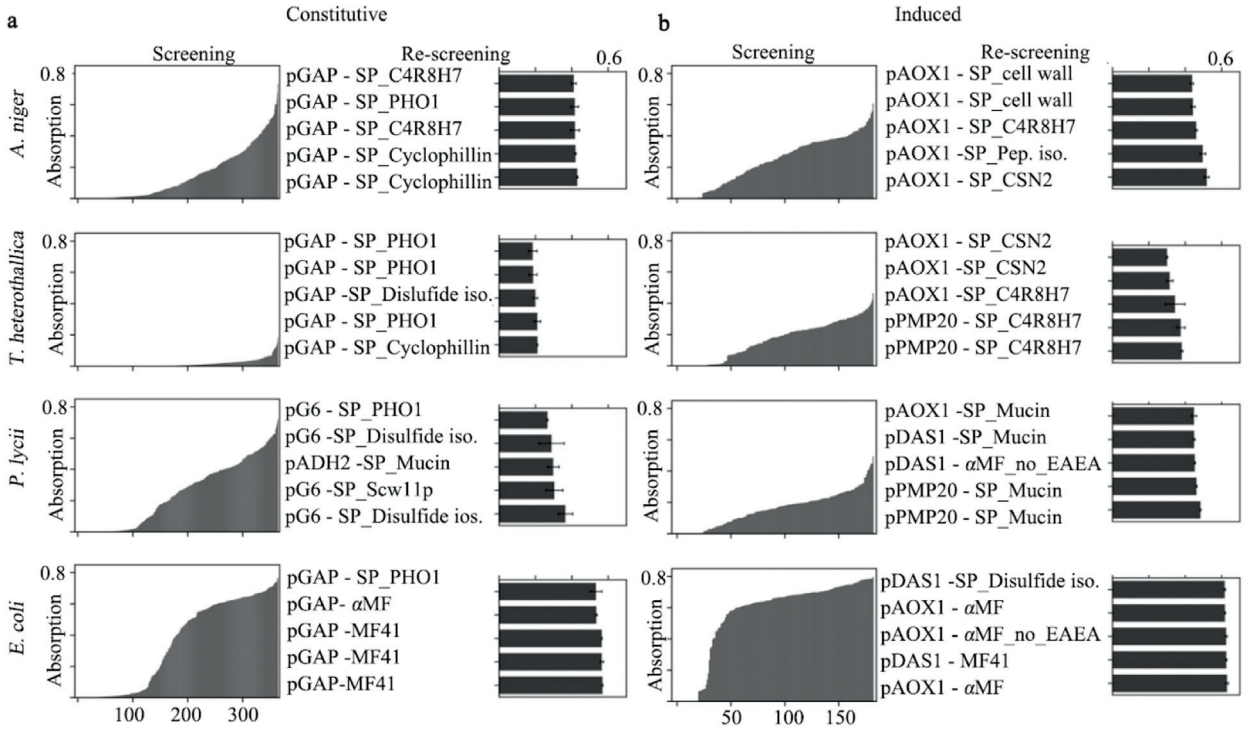

Fig. 3. Screening and Rescreening of phytases. For each phytase a screening for constitutive and induced expression was performed. Constitutive expression was performed in 2 % buffered glycerol-complex-phosphate buffer (BMGY-PP) and induced expression in 1 % buffered methanol-complex-phosphate buffer (BMMY-PP). To remove background noise, absorption values presented are measured absorption for each well subtracted by the average absorption of three medium controls which were assayed on each plate. The screening *x*-axis defines the number of samples screened in a ranked order. For each phytase, a re-screening of the constitutive and induced expression constructs was performed. Bars represent the mean absorption from the phytase assay of three biological replicates, subtracted by the mean absorption of three medium samples. Error bars denote ± 1 standard deviation. From the sequencing analysis, the genetic composition of promoter and secretion tag are indicated. *A.*: *Aspergillus; T.: Thielavia; P.*: *Peniophora.*

3.3. Shake flask cultivations for strain selection and media testing

In addition to the selection and combination of regulatory elements (strain design), different cultivation strategies (process design) greatly influence protein expression and secretion. Cultivation conditions often differ significantly between the initial screening and the final production process, which often makes scale-up challenging. Designing the overall process in a new system is essential to maximize yield and quality of phytase secretion (Looser et al., 2015). To demonstrate that the PTK can generate good producer strains, a single strain was selected for process optimization. For this, the 16 best performing strains were tested in shake flask format in two separate screenings. Based on the first screenings, a constitutive expression strain was chosen for methanol-free enzyme production, to prevent oxidative stress and special material handling, enable easier scale-up, and avoid protein degradation (Shen et al., 2016; Navone et al., 2021). The pGAP-MF41 AppA *E. coli* phytase construct was found multiple times in the shuffled screening as the best-performing constitutive strain. Other groups have reported similar observations, that AppA *E. coli* phytase is promising due to its characteristics (e. g., high temperature tolerance and high activity) and the good levels of expressed enzyme in *P. pastoris* (Chen et al., 2004). Hence, this strain was used further for phytase expression studies in shake flasks in complex medium as well as pure *Nostoc* sp. De1 hydrolysate using 2 % (*w/V*) glycerol or glucose as an additional carbon (C) source (Fig. 4). The composition of the *Nostoc* sp. De1 biomass and investigations of the enzymatic hydrolysis on the *Nostoc* sp. De1 biomass were reported by us before (Sinzinger et al., 2022).

The OD_{600} values of the cultures in BMGY and BMD were 23.7 and 18.9, respectively. The cultures did not grow as well in pure hydrolysate as they did in BMGY and BMD with OD_{600} of 18.8 and 14.3 (Fig. 4a). Little growth was observed in pure hydrolysate implying only very little readily available C-source. The phytase activity in BMGY and BMD reached 29.9 U/mL and 33.1 U/mL, respectively (Fig. 4b). In hydrolysate, the activities reached 23.6 U/mL and even 36.5 U/mL with glycerol and glucose as C-sources, respectively. Showing a tendency that glucose might be a good C-source for the expression system used here. The activities determined were still lower than the ones reported by others for the same *E. coli* phytase, e.g., by Akbarzadeh et al. (2015) who reached an activity of more than 200 U/mL with a pAOX1 system in modified BMGY after 96 h induction with methanol. Bai et al. (2009) reached a phytase activity of 243–412 U/mL over 48 h with a pGAP system depending on the medium composition. Shake flasks limit oxygen intake tremendously, which limits the interpretation of how well a producer strain can perform in a controlled system.

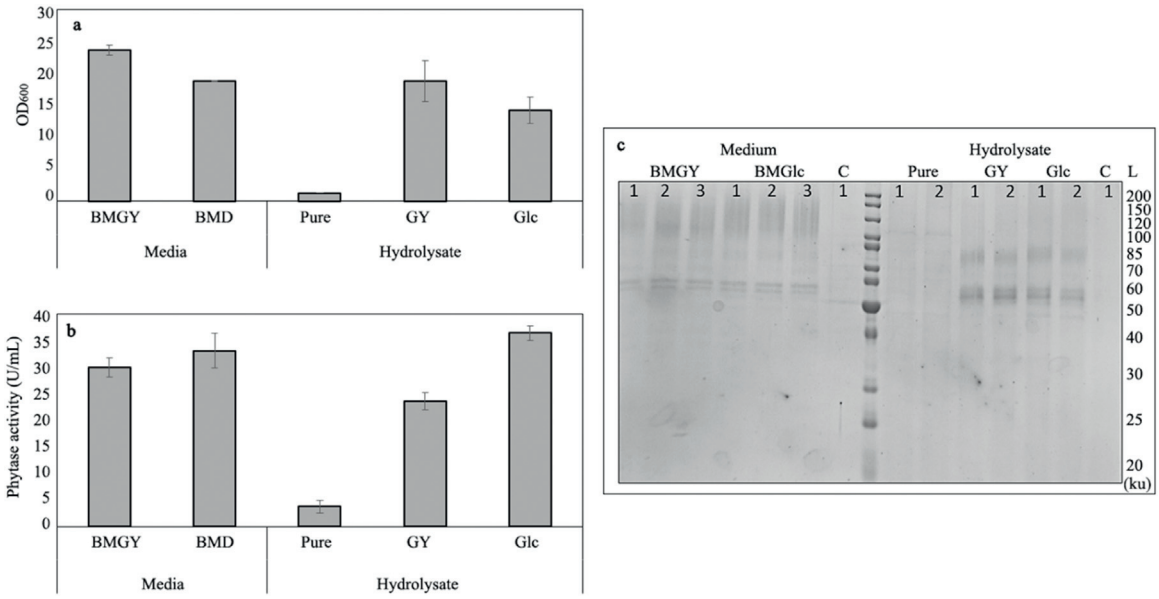

Fig. 4. Expression of pGAP-MF41 AppA *E. coli* phytase in 50 mL shake flasks. Expression in BMGY and BMD was done in triplicates, error bars showing ± 1 standard deviation. Expression in the *Nostoc* sp. De1 hydrolysate was done in duplicates as hydrolysate was limited, error bars showing relative deviation. (a) OD_{600} was measured after 48 h expression; (b) phytase activity was determined by colorimetric assay; (c) sodium dodecyl sulfate-polyacrylamide gel electrophoresis (SDS-PAGE) gel of the culture supernatants. The AppA *E. coli* phytase specific bands appearing at around 56 ku. C are medium controls. GY and Glc are the C-sources being glycerol and glucose, respectively. L is the protein ladder.

The presence of the protein was verified by sodium dodecyl sulfate–polyacrylamide gel electrophoresis (SDS-PAGE) analysis. In all relevant supernatants a clear band at the expected size of 56 ku was observed (Fig. 4c). This is in accordance with other results on this AppA *E. coli* phytase showing the same size of the protein and an unglycosylated native phytase with 45 ku (Chen et al., 2004). The bands in the samples with glycerol as a C-source were more prominent than with glucose in hydrolysate as well as the controlled complex medium. These larger bands might indicate higher enzyme concentrations in the hydrolysate samples, which are unmodified or improperly folded, potentially due to low oxygen availability in the shake flasks. Proceeding in a controlled system, glycerol as a C-source was considered for further testing to achieve higher activity.

3.4. Bench-top batch fermentation

The expression level of heterologous protein with pGAP is reported to be dependent on the protein itself, the medium, and the C-source (Karbalaei et al., 2020). A 1 L batch fermentation of (pGAP-MF41) AppA *E. coli* phytase was performed in BMGY medium as well as in 20 % (*V/V*) *Nostoc* sp. De1 hydrolysate (Fig. 5**)**. The fermentations in hydrolysate took almost twice as long as in BMGY. The final activities reached were about the same at over 500 U/mL. The growth and product kinetics in BMGY medium were better than in hydrolysate (Table 1).

The highest phytase activities in BMGY medium were achieved at 24 h (530 and 511 U/mL), while in *Nostoc* sp. De1 hydrolysate, the peak activities were observed at 28 h (522 and 528 U/mL). The BMGY reached the highest OD_{600} value of 112 after 18 h, with corresponding cell dry weights (CDWs) of 25 and 23 g/L. In the hydrolysate, the stationary phase was reached at 32 h, with OD_{600} values of 98 and CDWs of 19 and 20 g/L. Glycerol consumption slowed down after 18 h, indicating nutrient limitations due to dilution with deionized water. Despite this, phytase activity continued to increase until 48 h. Table 1 provides an overview of cultivation conditions and yields for batch and pulsed batch fermentation. The study demonstrates the potential use of 20 % *Nostoc* sp. De1 hydrolysate as a fermentation medium for AppA *E. coli* phytase. The utilization of cyanobacterial hydrolysate thus could be a key in the development of cyanobacterial biorefinery concepts and associated cost economics. Although cyanobacteria are regarded as promising renewable feedstock, the main economic challenges of cyanobacterial biorefineries today are the still low concentration of products and high costs of cultivation and product recovery. Economic analysis such as the study of Fasahati et al. (2019) report a large span of costs for cyanobacterial products depending on the product type, e.g., in the range of 2.74–34.00 US dollar per kg based on product concentrations of 0.5 g/L in open pond cultivation systems. With respect to this, among other demands for improvement, a multiproduct approach including value added utilization even of the residual biomass is of high importance to add the most possible value to such a process. The utilization of cyanobacterial biomass for fermentation medium is to be seen as part of such a strategy.

Further, we aimed to develop a fed-batch bioprocess for AppA *E. coli* phytase in BMGY. Initially, the maximum specific growth rate μ_{max} (1/h) was determined by pulsed-batch fermentation of *P. pastoris* in BMGY (Fig. 5c). Pulses of additional C-source were performed with 25 g/L of glycerol into the fermentation broth after 15 h. The fermentation resulted in a maximum activity of

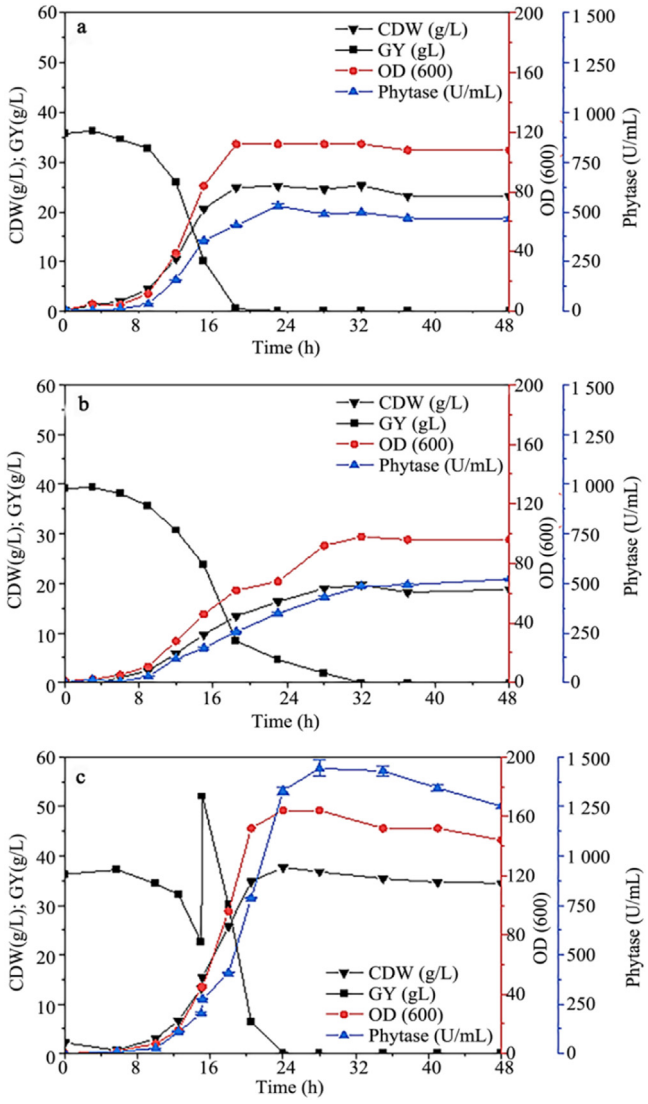

Fig. 5. The *P. pastoris* fermentation constitutively expressing pGAP-MF41 AppA *E. coli* phytase in a 1 L system over 48 h. (a) the batch fermentation in 4 % BMGY; (b) in 20 % (*V/V*) *Nostoc* sp. De1 biomass hydrolysate in *di*H_2O, hydrolysate was produced enzymatically as described in the text; (c) a pulsed-batch fermentation in 4 % BMGY. The glycerol pulse was done as described in the text. Phytase activity is shown as mean of analytical triplicates with one standard deviation. CDW: cell dry weight.

around 1 450 U/mL, which is 2.5-fold higher than the maximum yield obtained with previous batch fermentations run in BMGY. The maximum cell dry weight was around 1.5-fold higher than in the batch fermentations. Most growth and product kinetics, such as the maximum activity formation rate $q_{A,max}(\mu)$, improved when applying the pulsed batch fermentation strategy. The $q_{A,max}$ (μ) increased by more than 30 %, thereby showing that no system limitations were constraining the phytase expression at this point. For a more dynamic process, a second glycerol pulse could be applied to explore the limitations of the bioreactor system early in the process development (Looser et al., 2015). An overview of the determined growth and product kinetics of the conducted batch and pulsed batch fermentation is also shown in Table 1.

Contrary to induced expressions for high-cell density fermentation with three phases (batch phase, fed-batch phase, and induction phase), constitutive expression consists of just two: batch and fed-batch phase (Liu et al., 2019). Hence, the product formation in the fed-batch phase must be specifically tailored to the expression host and the reactor system. The key parameter to be determined for a high yield strategy is the specific productivity $\mu(q_A)$ the product of specific growth rate μ and product formation rate q_A. Hence, it must be investigated to determine the ideal feed rate for an exponential feed strategy. The $\mu(q_{A,max})$ and μ_{max} for the pulsed batch fermentations were determined to be the same with μ_{max} corresponding to a doubling time of 2.5 h. Contrary to induced expressions, which usually show to have their $\mu(q_{A,max})$ close to zero growth on methanol. Reported $\mu(q_{A,max})$ for pGAP regulated constitutive expression were usually just below μ_{max}.

Table 1
Overview of cultivation conditions, growth kinetics and products kinetics of periplasmic phosphoanhydride phosphatase (AppA) *Escherichia coli* phytase production with *Pichia pastoris* in a 1 L system using glycerol for C-source.

Cultivation condition						Growth kinetics				Product kinetics			
Medium	Temperature (°C)	pH	Mode	S_{total} (g/L)	Time (h)	CDW_{max} (g/L)	$Y_{x/s}$ (g/g)	$q_{s,max}$ (g/(g·h))	μ_{max} (1/h)	$A_{p,max}$ (U/mL)	$Y_{A/x,max}$ (U/g)	$q_{A,max}$ (U/(g·h))	$\mu(q_{A,max})$ (1/h)
BMGY	30	6.0	Batch	40	24	25. 3	0.70	0.72	0.286	530.0	21 378	6 680	0.286
BMGY	30	6.0	Batch	40	24	23. 4	0.59	0.84	0.266	522.0	23 337	6 536	0.266
BMGY	30	6.0	Pulsed Batch	65	28	36.6	0.58	1.10	0.303	1 458.6	42 034	17 515	0.303
BMGY	30	6.0	Pulsed Batch	65	28	37.7	0.57	1.04	0.308	1 342.9	40 395	14 281	0.308
20 % Hydrol.	30	6.0	Batch	40	32	19.7	0.50	1.18	0.300	522.3	27 182	8 408	0.300
20 % Hydrol.	30	6.0	Batch	40	32	19.0	0.48	1.16	0.170	528.3	30 016	1 432	0.170

Notes: The growth and product kinetics were used for the determination of feeding parameters to develop a fed-batch strategy. The hydrolysate was produced from *Nostoc* sp. *De1* biomass. S_{Total}, total substrate; CDW, cell dry weight; $Y_{x/s}$, biomass yield per substrate; q_s, substrate utilization rate; μ, growth rate; A_p, activity yield; $Y_{A/X}$, activity yield per biomass; $q_A(\mu)$, specific product formation rate; $\mu(q_A)$, specific growth rate.

3.5. Fed-batch strategy development

The exponential feed rate for high cell density fermentation of *P. pastoris* requires an ideal C-source feed rate. The μ_{max} of 0.3, determined from a pulsed batch fermentation, served as the exponential feed rate and 75 % of this μmax was also tested. Glycerol feed was limited by bioreactor space, with 4 % (*w*/*V*) starting glycerol and an additional 0.2 L of 50 % (*w*/*V*) glycerol solution fed. However, glycerol started accumulating due to the limited capacity of the 1 L system to sustain the organism's high growth rate. Fermentation curves are shown in Fig. 6a (μ_{max}) and 6b (75 % μ_{max}). The maximum activity yield and activity yield per biomass with exponential feeds were around 3 400 U/mL and 59 000 U/g for μ_{max} feed, and over 3 800 U/mL and 76 000 U/g for 75 % μ_{max} feed. Maximum CDW close to 100 g/L was achieved just before glycerol was completely consumed. Phytase activity, especially in μ_{max} feed fermentations, was strongly affected by glycerol accumulation, with a larger drop in activity after approximately 40 h of fermentation. Table 2 compares cultivation conditions, growth, and product kinetics for all fed-batch fermentations.

A notable difference between the two exponential feeds was that glycerol was temporarily consumed between 20 and 26 h in the 75 % μ_{max} feed fermentations, leading to a rise in dissolved oxygen levels. In contrast, dissolved oxygen dropped to zero until complete glycerol consumption in μmax feed fermentations. The low growth rates after 20 h resulted in decreased $q_A(\mu)$ values, indicating limited biomass formation and enzyme expression due to oxygen availability. However, the DO-stat strategy demonstrated lower oxidative stress.

The high cell density fermentation with exponential feed exhibited high phytase activity after 24 h, with minimal increase thereafter. To further increase phytase yield in the 1 L system, a DO-stat fermentation strategy was employed, maintaining DO above 20 %. Two DO-thresholds were tested: 30 % and 20 % DO (Fig. 6c and 6d), reaching over 4 000 U/mL. Glycerol levels were maintained at zero throughout the fed batch phase but DO-stat fermentations took 5–10 h longer than exponential feed strategy fermentations and yielded 20 %–25 % lower biomass (CDW) and max biomass per substrate yields. Growth slowed down after 30 h, particularly in DO-stat fermentations with a 20 % DO-threshold. Significant drops in enzyme activity were observed after approximately 40 h, possibly due to cellular proteases released from *P. pastoris* cells. The change from exponential feed to DO-stat feed strategy reduced growth kinetics but improved product kinetics. Although $q_{A,max}(\mu)$ decreased by more than 100 %, the maximum activity yield increased by more than 20 %. The DO-stat feed with a 30 % threshold showed promising results, with maximum activity yields of around 4 000 U/mL and activity yield per biomass over 4 400 U/g.

The DO-stat controlled feed strategy proved more effective than the exponential feed strategy for *P. pastoris* in a 1 L system, particularly with a 30 % DO threshold. Modifications were made by adjusting the DO-cascade, regulating aeration, agitation, and oxygen supply ratio. The 1 L system provided a maximum air flow of 50 sL/h, allowing for high aeration of 1–1.2 ($m^3/(m^3 \cdot min)$). To minimize protease release, the stir rate was reduced from 1200 rpm to 900 r/min (Fig. 6e). Additionally, a lower fermentation temperature of 25 °C after 12 h was implemented (Fig. 6f).

The modified DO-stat controlled feed strategy with a 30 % threshold, 1–1.2 ($m^3/(m^3 \cdot min)$), and 900 r/min showed improved fermentation results overall. While it did not reach the maximum space-time yield of exponential feed fermentations, it significantly improved activity yields per biomass. The maximum activity yield and activity yield per biomass increased by up to 40 %, reaching 7 200 U/mL and 113 000 U/g after 77 h fermentation, respectively. The lower temperature of 25 °C also resulted in around a 30 % increase in activity yield compared to the non-optimized DO-stat strategy. Studies of other authors on *P. pastoris* fermentation producing *E. coli* phytase ranged from 112.5 U/mL after 72 h in shake flasks to 30 246 U/mL after 180 h in a 50-L fermenter (Tai et al., 2013; Helian et al., 2020). However, the comparison is somewhat limited, as fermentation systems of different laboratories usually have different set-ups and limitations. Limited oxygen supply by the aeration system was an issue in the fermentation system available in our laboratories, which certainly limits activity yields. Yet, our results are very promising. Investigations on expressions in a larger-

Table 2
Overview of cultivation conditions, growth kinetis, and product kinetics of the conducted AppA (periplasmic phosphoanhydride phosphatase) *E. coli* phytase production with *P. pastoris*, namely exponential feed with feed for μ_{max} and 75 % of μ_{max}, DO-*stat* feed with 20 % and 30 % DO-limits, and optimized DO-*stat* feed strategies with reduced stirring rate and increased aeration.

Cultivation condition							Growth kinetics				Product kinetics			
Mode	Temperature (°C)	pH	DO-lvl (%)	Stirring rate (r/min)	Air ($m^3/(m^3 \cdot min)$)	S_{total} (g)	CDW_{max} (g/L)	$Y_{x/s}$ (g/g)	$q_{s,max}$ (g/(g·h))	μ_{max} (1/h)	$A_{p,\ max}$ (U/mL)	$Y_{A/x,\ max}$ (U/g)	$q_{A,max}$ (μ) (U/(g·h))	STY_{max} (U/(L·h))
Exp. Feed μ_{max}	30	6.0	30	400–1 200	0.2–0.5	240	98.8	0.45	142.32	0.246	3,435	59,677	18,090	130,357
Exp. Feed μ_{max}	30	6.0	30	400–1 200	0.2–0.5	240	99.4	0.45	6.74	0.281	3,432	55,940	16,538	128,705
Exp. Feed 75 % μ_{max}	30	6.0	30	400–1 200	0.2–0.5	240	97.5	0.45	1.56	0.357	3,573	76,197	17,522	116,709
Exp. Feed 75 % μ_{max}	30	6.0	30	400–1 200	0.2–0.5	240	96.5	0.44	16.47	0.272	3,880	76,459	16,546	118,518
DO-*stat* (20 %)	30	6.0	30	400–1200	0.2–0.5	240	77.5	0.35	0.59	0.249	4,093	59,293	6,012	81,324
DO-*stat* (20 %)	30	6.0	30	400–1 200	0.2–0.5	240	77.9	0.36	0.61	0.258	3,950	58,337	5,628	79,348
DO-*stat* (30 %)	30	6.0	30	400–1 200	0.2–0.5	240	77.5	0.36	0.57	0.274	4,446	75,449	8,657	96,661
DO-stat (30 %)	30	6.0	30	400–1 200	0.2–0.5	240	75.5	0.35	0.63	0.227	4,177	67,614	8,151	82,458
DO-*stat* (30 %)	30	6.0	30	400–900	1.0-1.2	240	72.4	0.33	0.46	0.186	6,531	104,686	8,622	102,903
DO-*stat* (30 %)	30	6.0	30	400–900	1.0–1.2	240	72.9	0.33	0.42	0.207	7,213	113,337	8,222	93,681
DO-*stat* (30 %)	25	6.0	30	400–900	1.0–1.2	240	97.8	0.45	0.42	0.155	6,317	76,305	4,850	82,042
DO-*stat* (30 %)	25	6.0	30	400–900	1.0–1.2	240	101.6	0.46	0.41	0.230	5,671	60,100	4,050	73,660

Notes: S_{total}, total substrate; CDW, cell dry weight; $Y_{x/s}$: biomass yield per substrate; q_s, substrate utilization rate; μ, growth rate; A_p, activity yield; $Y_{A/X}$, activity yield per biomass; $q_A(\mu)$, specific product formation rate; STY, space time yield.

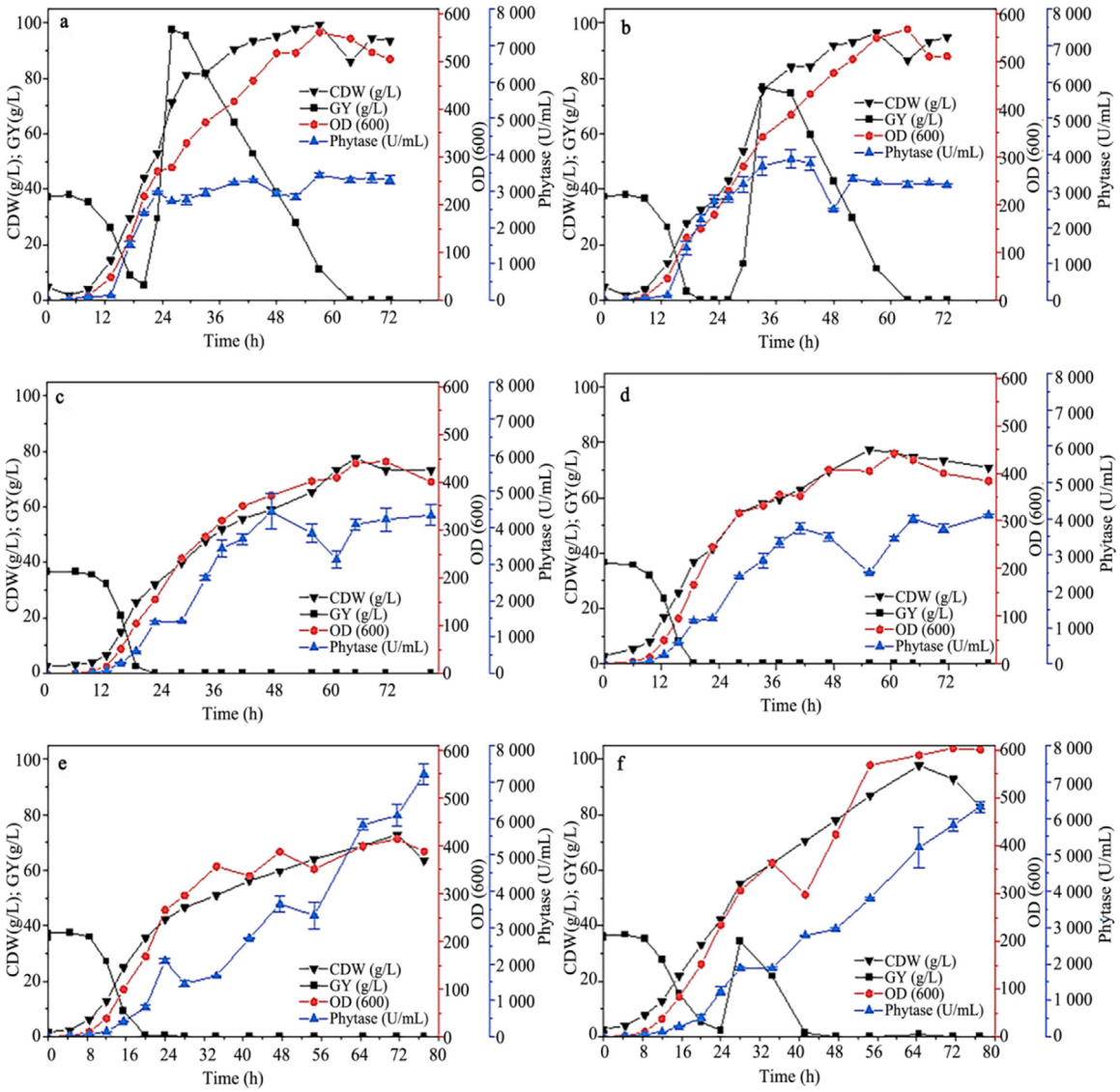

Fig. 6. Fed-batch development of *P. pastoris* fermentation constitutively expressing pGAP-MF41 AppA *E. coli* phytase in a 1 L fermenter system with 4 % BMGY medium feeding 200 g glycerol. We started with an exponential feed based on the calculated μ_{max} from batch and pulsed batch fermentations shown in (a) and a feed based on 75 % of μ_{max} in (b). The following step was a DO-stat feeding strategy with 30 % dissolved oxygen limit shown in (c) and 20 % dissolved oxygen limit in (d). The next step was improving the DO-cascade by lowering the max stir rate from 1 200 to 900 r/min and increasing the aeration to its maximum around 1.2 ($m^3/(m^3 \cdot min)$) shown in (e) and a decrease of temperature from 30 to 25 °C in (f).

scale system with better aeration and lower starting volume, ought to be done to further elucidate the potential of the strain developed in this study.

4. Conclusions

We applied a multi-field research approach to a *P. pastoris* enzyme production platform showing the potential to use cyanobacterial biomass as feedstock. We characterized and extended a combinatorial library to facilitate *P. pastoris* engineering, characterized the library components, and screened libraries for industrially relevant enzyme production. We developed a fed-batch strategy for AppA *E. coli* phytase expression and successfully demonstrated the utilization of *Nostoc* sp. De1 biomass hydrolysate. Thus, we could show that the extended *P. pastoris* toolkit can produce relevant producer strains and the enzyme expression with cyanobacterial biomass as feedstock may be an industrially relevant and more sustainable alternative to currently used sources. Global challenges, such

as economically feasible biobased production, will require creative solutions. This work highlights the value of multidisciplinary approaches to these issues and demonstrates how new biotechnologies can fuel novel solutions.

Declaration of Competing Interest

There are no conflicts to declare.

Acknowledgment

The EFRE—Interreg project 41 “Joint Research on Natural Compounds from Cyanobacteria as a Model of Cross-Border Scientific Partnership” was funded by the European Union ZIEL ETZ. Many thanks to Algatech for providing the biomass and to Prof. Timothy K. Lu (MIT) for providing *P. pastoris attP*.

Supplementary materials

Supplementary material associated with this article can be found, in the online version, at doi:10.1016/j.jobab.2023.12.005.

References

Akbarzadeh, A., Dehnavi, E., Aghaeepoor, M., Amani, J., 2015. Optimization of recombinant expression of synthetic bacterial phytase in *Pichia pastoris* using response surface methodology. Jundishapur J. Microbiol. 8, e27553.
Bae, H.D., Yanke, L.J., Cheng, K.J., Selinger, L.B., 1999. A novel staining method for detecting phytase activity. J. Microbiol. Methods 39, 17–22.
Bai, Y.G., Yang, P.L., Wang, Y.R., Shi, P.J., Luo, H.Y., Meng, K., Wu, B., Yao, B., 2009. Phytase production by fermentation of recombinant *Pichia pastoris* in monosodium glutamate wastewater. World J. Microbiol. Biotechnol. 25, 1643–1649.
Briones-Nagata, M.P., Martinez-Goss, M.R., Hori, K., 2007. A comparison of the morpho-cytology and chemical composition of the two forms of the cyanobacterium, *Nostoc* commune Vauch., from the Philippines and Japan. J. Appl. Phycol. 19, 675–683.
Canton, B., Labno, A., Endy, D., 2008. Refinement and standardization of synthetic biological parts and devices. Nat. Biotechnol. 26, 787–793.
Celińska, E., Borkowska, M., Białas, W., Korpys, P., Nicaud, J.M., 2018. Robust signal peptides for protein secretion in *Yarrowia lipolytica*: identification and characterization of novel secretory tags. Appl. Microbiol. Biotechnol. 102, 5221–5233.
Chandra, R., Iqbal, H.M.N., Vishal, G., Lee, H.S., Nagra, S., 2019. Algal biorefinery: a sustainable approach to valorize algal-based biomass towards multiple product recovery. Bioresour. Technol. 278, 346–359.
Chen, C.C., Cheng, K.J., Ko, T.P., Guo, R.T., 2015. Current progresses in phytase research: three-dimensional structure and protein engineering. ChemBioEng Rev. 2, 76–86.
Chen, C.C., Wu, P.H., Huang, C.T., Cheng, K.J., 2004. A *Pichia pastoris* fermentation strategy for enhancing the heterologous expression of an *Escherichia coli* phytase. Enzyme Microb. Technol. 35, 315–320.
Choi, S.P., Nguyen, M.T., Sim, S.J., 2010. Enzymatic pretreatment of *Chlamydomonas reinhardtii* biomass for ethanol production. Bioresour. Technol. 101, 5330–5336.
Curran, K.A., Karim, A.S., Gupta, A., Alper, H.S., 2013. Use of expression-enhancing terminators in *Saccharomyces cerevisiae* to increase mRNA half-life and improve gene expression control for metabolic engineering applications. Metab. Eng. 19, 88–97.
David, G., 2018. Chapter 26—economics of food and feed enzymes: status and prospectives. In: Enzymes in Human and Animal Nutrition. Academic Press, USA, pp. 487–514.
de Farias Silva, C.E., Barbera, E., Bertucco, A., 2019. Biorefinery as a promising approach to promote ethanol industry from microalgae and Cyanobacteria. Bioethanol Production from Food Crops. Elsevier, Amsterdam, pp. 343–359.
Delic, M., Valli, M., Graf, A.B., Pfeffer, M., Mattanovich, D., Gasser, B., 2013. The secretory pathway: exploring yeast diversity. FEMS Microbiol. Rev. 37, 872–914.
Engler, C., Gruetzner, R., Kandzia, R., Marillonnet, S., 2009. Golden gate shuffling: a one-pot DNA shuffling method based on type IIs restriction enzymes. PLoS One 4, e5553.
Fasahati, P., Wu, W.Z., Maravelias, C.T., 2019. Process synthesis and economic analysis of cyanobacteria biorefineries: a superstructure-based approach. Appl. Energy 253, 113625.
Han, Y.M., Lei, X.G., 1999. Role of glycosylation in the functional expression of an*Aspergillus niger*Phytase (*phyA*) in*Pichia pastoris*. Arch. Biochem. Biophys. 364, 83–90.
Helian, Y.K., Gai, Y.M., Fang, H., Sun, Y.M., Zhang, D.W., 2020. A multistrategy approach for improving the expression of *E. coli* phytase in *Pichia pastoris*. J. Ind. Microbiol. Biotechnol. 47, 1161–1172.
Herrmann, K.R., Ruff, A.J., Infanzón, B., Schwaneberg, U., 2019. Engineered phytases for emerging biotechnological applications beyond animal feeding. Appl. Microbiol. Biotechnol. 103, 6435–6448.
Hesampour, A., Siadat, S.E.R., Malboobi, M.A., Mohandesi, N., Arab, S.S., Ghahremanpour, M.M., 2015. Enhancement of thermostability and kinetic efficiency of *Aspergillus niger* PhyA phytase by site-directed mutagenesis. Appl. Biochem. Biotechnol. 175, 2528–2541.
Karbalaei, M., Rezaee, S.A., Farsiani, H., 2020. *Pichia pastoris*: a highly successful expression system for optimal synthesis of heterologous proteins. J. Cell. Physiol. 235, 5867–5881.
Lee, M.E., DeLoache, W.C., Cervantes, B., Dueber, J.E., 2015. A highly characterized yeast toolkit for modular, multipart assembly. ACS Synth. Biol. 4, 975–986.
Liang, S.L., Li, C., Ye, Y.R., Lin, Y., 2013. Endogenous signal peptides efficiently mediate the secretion of recombinant proteins in *Pichia pastoris*. Biotechnol. Lett. 35, 97–105.
Liu, W.C., Inwood, S., Gong, T., Sharma, A., Yu, L.Y., Zhu, P., 2019. Fed-batch high-cell-density fermentation strategies for *Pichia pastoris* growth and production. Crit. Rev. Biotechnol. 39, 258–271.
Looser, V., Bruhlmann, B., Bumbak, F., Stenger, C., Costa, M., Camattari, A., Fotiadis, D., Kovar, K., 2015. Cultivation strategies to enhance productivity of *Pichia pastoris*: a review. Biotechnol. Adv. 33, 1177–1193.
Madden, K., Tolstorukov, I., Cregg, J., 2015. In: Electroporation of *Pichia pastoris*. Genetic Transformation Systems in Fungi, 1. Springer, Cham, pp. 87–91 2015.
Massahi, A., Çalık, P., 2015. In-silico determination of *Pichia pastoris* signal peptides for extracellular recombinant protein production. J. Theor. Biol. 364, 179–188.
Mitra, M., Mishra, S., 2019. Multiproduct biorefinery from *Arthrospira* spp. towards zero waste: current status and future trends. Bioresour. Technol. 291, 121928.
Möllers, K.B., Cannella, D., Jørgensen, H., Frigaard, N.U., 2014. Cyanobacterial biomass as carbohydrate and nutrient feedstock for bioethanol production by yeast fermentation. Biotechnol. Biofuels 7, 64.
Morse, N.J., Gopal, M.R., Wagner, J.M., Alper, H.S., 2017. Yeast *Terminator* function can be modulated and designed on the basis of predictions of nucleosome occupancy. ACS Synth. Biol. 6, 2086–2095.
Navone, L., Vogl, T., Luangthongkam, P., Blinco, J.A., Luna-Flores, C., Chen, X.J., von Hellens, J., Speight, R., 2021. Synergistic optimisation of expression, folding, and secretion improves *E. coli* AppA phytase production in *Pichia pastoris*. Microb. Cell Fact. 20, 8.
Obst, U., Lu, T.K., Sieber, V., 2017. A modular toolkit for generating *Pichia pastoris* secretion libraries. ACS Synth. Biol. 6, 1016–1025.
Perez-Pinera, P., Han, N.R., Cleto, S., Cao, J.C., Purcell, O., Shah, K.A., Lee, K., Ram, R., Lu, T.K., 2016. Synthetic biology and microbioreactor platforms for programmable production of biologics at the point-of-care. Nat. Commun. 7, 12211.

Prielhofer, R., Barrero, J.J., Steuer, S., Gassler, T., Zahrl, R., Baumann, K., Sauer, M., Mattanovich, D., Gasser, B., Marx, H., 2017. GoldenPiCS: a Golden Gate-derived modular cloning system for applied synthetic biology in the yeast *Pichia pastoris*. BMC Syst. Biol. 11, 123.

Prielhofer, R., Maurer, M., Klein, J., Wenger, J., Kiziak, C., Gasser, B., Mattanovich, D., 2013. Induction without methanol: novel regulated promoters enable high-level expression in *Pichia pastoris*. Microb. Cell Fact. 12, 5.

Qin, X., Qian, J., Xiao, C., Zhuang, Y., Zhang, S., Chu, J., 2011. Reliable high-throughput approach for screening of engineered constitutive promoters in the yeast *Pichia pastoris*. Lett. Appl. Microbiol. 52, 634–641.

Rajkumar, A.S., Varela, J.A., Juergens, H., Daran, J.MG., Morrissey, J.P., 2019. Biological parts for *Kluyveromyces marxianus* synthetic biology. Front. Bioeng. Biotechnol. 7, 97.

Ranjan, B., Satyanarayana, T., 2016. Recombinant HAP phytase of the thermophilic mold *Sporotrichum thermophile:* expression of the *Codon*-optimized phytase gene in *Pichia pastoris* and applications. Mol. Biotechnol. 58, 137–147.

Shen, W., Xue, Y., Liu, Y.Q., Kong, C.X., Wang, X.L., Huang, M.M., Cai, M.H., Zhou, X.S., Zhang, Y.X., Zhou, M., 2016. A novel methanol-free *Pichia pastoris* system for recombinant protein expression. Microb. Cell Fact. 15, 178.

Sinzinger, K., Schieder, D., Rühmann, B., Sieber, V., 2022. Towards a cyanobacterial biorefinery: carbohydrate fingerprint, biocomposition and enzymatic hydrolysis of *Nostoc* biomass. Algal Res. 65, 102744.

Stadlmayr, G., Mecklenbräuker, A., Rothmüller, M., Maurer, M., Sauer, M., Mattanovich, D., Gasser, B., 2010. Identification and characterisation of novel *Pichia pastoris* promoters for heterologous protein production. J. Biotechnol. 150, 519–529.

Tai, H.M., Yin, L.J., Chen, W.C., Jiang, S.T., 2013. Overexpression of *Escherichia coli* phytase in *Pichia pastoris* and its biochemical properties. J. Agric. Food Chem. 61, 6007–6015.

Vogl, T., Sturmberger, L., Kickenweiz, T., Wasmayer, R., Schmid, C., Hatzl, A.M., Gerstmann, M.A., Pitzer, J., Wagner, M., Thallinger, G.G., Geier, M., Glieder, A., 2016. A toolbox of diverse promoters related to methanol utilization: functionally verified parts for heterologous pathway expression in *Pichia pastoris*. ACS Synth. Biol. 5, 172–186.

Weis, R., Luiten, R., Skranc, W., Schwab, H., Wubbolts, M., Glieder, A., 2004. Reliable high-throughput screening with *Pichia pastoris* by limiting yeast cell death phenomena. FEMS Yeast Res. 5, 179–189.

Xiong, A.S., Yao, Q.H., Peng, R.H., Han, P.L., Cheng, Z.M., Li, Y., 2005. High level expression of a recombinant acid phytase gene in *Pichia pastoris*. J. Appl. Microbiol. 98, 418–428.

Yarimizu, T., Nakamura, M., Hoshida, H., Akada, R., 2015. Synthetic signal sequences that enable efficient secretory protein production in the yeast *Kluyveromyces marxianus*. Microb. Cell Fact. 14, 20.

Zang, J.K., Zhu, Y.F., Zhou, Y., Gu, C.J., Yi, Y.F., Wang, S.X., Xu, S.Q., Hu, G.W., Du, S.J., Yin, Y.N., Wang, Y.L., Yang, Y., Zhang, X.Y., Wang, H.K., Yin, F.F., Zhang, C., Deng, Q., Xie, Y.H., Huang, Z., 2021. Yeast-produced RBD-based recombinant protein vaccines elicit broadly neutralizing antibodies and durable protective immunity against SARS-CoV-2 infection. Cell Discov. 7, 71.